

Quantum-classical correspondence in the wavefunctions of Andreev billiards

A. Kormányos,^{1,*} Z. Kaufmann,² J. Cserti,² and C. J. Lambert¹

¹*Department of Physics, Lancaster University, Lancaster, LA1 4YB, UK*

²*Department of Physics of Complex Systems, Eötvös University,
H-1117 Budapest, Pázmány Péter sétány 1/A, Hungary*

We present a classical and quantum mechanical study of an Andreev billiard with a chaotic normal dot. We demonstrate that in general the classical dynamics of these normal-superconductor hybrid systems is mixed, thereby indicating the limitations of a widely used retracing approximation. We show that the mixed classical dynamics gives rise to a wealth of wavefunction phenomena, including periodic orbit scarring and localization of the wavefunction onto other classical phase space objects such as intermittent regions and quantized tori.

PACS numbers: 74.45.+c, 75.45.+j, 03.65.Sq

Wavefunction phenomena in closed and open quantum dot systems have attracted much attention in recent years. Besides the ongoing theoretical interest in a simple yet detailed description of scarring[1, 2], a range of phenomena have been studied including the connection between conductance oscillations, transmission resonances of ballistic semiconductor dots and microwave cavities, light emission from dielectric cavities and the localization of the wavefunction onto classical phase space objects[3] such as Kolmogorov-Arnold-Moser (KAM) islands[4], hierarchical regions[5] and periodic orbits[6]. It has been also pointed out, that certain states of a closed quantum dot, associated with KAM islands or bouncing-ball trajectories, actually survive the coupling of the dot to external leads, since level broadenings are not uniform, and this can give rise to measurable transport effects[7].

Systems consisting of a ballistic quantum dot coupled to a superconductor, which are commonly called Andreev-billiards (ABs)[8, 9] raise new questions of quantum-classical correspondence addressed by only a few works [10, 11, 12, 13, 14] beforehand. The key physical process taking place in normal-superconductor (N-S) hybrid nanostructures is the Andreev reflection[15], whereby electron-like quasi-particles with energies $E_F + \varepsilon$ (E_F is the Fermi energy) are coherently scattered into Fermi sea holes of energy $E_F - \varepsilon$ (and vice versa) at the N-S interface if ε is smaller than the superconducting gap Δ . For $\varepsilon = 0$ the Andreev reflected electrons (holes) perfectly retrace their classical trajectories as holes (electrons). For $\varepsilon > 0$ the velocities of the quasiparticles are not exactly reversed because of the 2ε difference in their energies, but this is not considered in most of the literature.

The validity of this widely used retracing approximation is questionable for ABs with chaotic normal dots, if the time between two Andreev-reflections is significantly longer than the ergodic time, because the small misalignment between the velocities of the electrons and holes at the N-S interface leads eventually to divergent trajectories. One notable exception, in which the consequences of the non-exact velocity reversal were investigated is the

paper by Silvestrov et al. [10]. They studied an Andreev-billiard with a chaotic normal dot and found that even though the motion in the normal dot could be characterized by non-zero Lyapunov-exponents, the existence of an adiabatic invariant in the N-S system to good approximation confines the electron-hole orbits to tori. Nevertheless, the exponential divergence of nearby trajectories does manifest itself through a gap in the low energy density of states (DOS) and through the eigenfunctions of the system, which were predicted to exhibit a peculiar localization property, different from those known in normal billiards. However, no quantum calculations were performed to support the latter finding.

Recently, Wiersig [16] has shown that the diffraction occurring at the points separating the normal and superconducting segments of the dot boundary (coined “critical points”) also plays an important role in the classical dynamics of ABs. Electrons (holes) hitting the boundary at nearby points belonging to different types of segment will undergo either Andreev or normal reflection and will be scattered into different quasi-particle states (ie into holes or electrons). Owing to the special geometry this diffraction effect was not observed in Ref. [10].

In this Letter we show, that in a more general case, the interplay of the *non-exact velocity reversal* and the *diffraction* at the critical points leads to the breakup of the (adiabatic) tori in at least certain parts of the phase space [see Fig. 1(a),(b)] rendering the classical dynamics mixed. While it has been known for a long time, that an applied magnetic field can render the ABs (weakly) chaotic[8, 14], to our knowledge the possibility that the dynamics of ABs can be irregular even for zero magnetic field has not yet been addressed in the literature. We argue moreover that the combination of these two effects results in a wealth of phenomena not only in the classical but also in the quantum dynamics of ABs. What makes these N-S hybrid systems additionally interesting and novel in the realm of quantum chaos studies is that the wavefunction is spinor and not scalar, as in normal billiards. We calculate, for the first time, the exact quantum eigenfunctions of a two dimensional AB with chaotic

normal dot. Using the Wigner transform of the eigenstates we find that most of them can be associated either with the regular or the chaotic regions of the energy surface.

The particular system used in our numerical calculations is the Sinai-Andreev (SA) billiard[19]. It consists of a Sinai-billiard shaped normal dot and an attached (infinite) superconducting lead (see Fig. 1(c) for the geometry). First, we consider the classical dynamics.

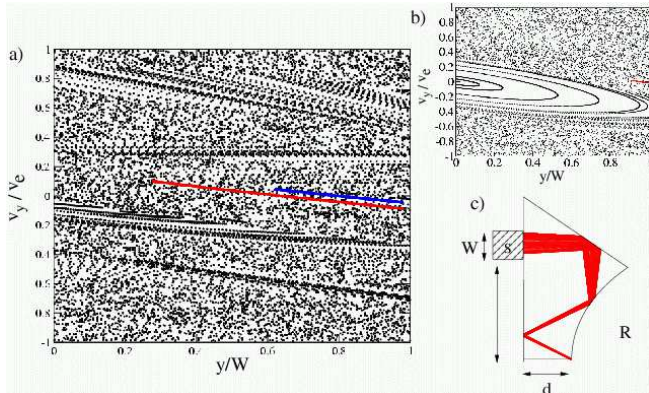


FIG. 1: (color online) The Poincaré section of the SA billiard for $h = 0.58$ (a) and $h = 0$ (b). (For other parameters see [27]). Each dot represents a starting point of an electron trajectory; the red and blue dots correspond to very elongated regular islands. The torus shown with red dots in (a) is projected onto real space (c).

Fig. 1(a,b) shows the Poincaré section (PS) which is defined as follows. The coordinates of each point in PS are the position y of the electron starting from the N-S interface and the tangential velocity component v_y in units of $v_e = v_F \sqrt{1 + \varepsilon/E_F}$, where v_F is the Fermi velocity (y is measured from the lower corner of the N-S interface). As can be observed, the PS resembles the Poincaré maps of generic normal systems with mixed classical dynamics. In large regions of the energy surface the motion is *chaotic*, while *islands of stability* are preserved only around such unstable periodic orbits of the isolated normal system, which hit the N-S interface at right angle. We emphasize that in contrast to Ref. [10], these phase space structures are regular islands not only in the adiabatic approximation. Depending on the instability of the orbit and the value of ε/E_F , the presence of the superconductor can indeed stabilize the motion, as can be checked by computing the stability matrix of the corresponding electron-hole orbit. Most of these islands are extremely elongated (see eg Fig. 1(a,b), where they are denoted by red and blue dots). Moreover, considering the bunch of electron trajectories lying on a particular torus, its projection onto the real space is “squeezed down” away from the N-S interface [Fig. 1(c)]. Both phenomena are consequences of the exponential divergence of nearby trajectories in the normal dot[10]. For islands centered on the least unstable orbits (eg the one at $h = 0$) these effects

are less pronounced [see the large island in Fig. 1(b)].

Furthermore, strips of regular, *intermittent-like* motions can also be observed in Fig. 1(a), in particular around $v_y/v_e \approx 0.7, 0.3, -0.2$, and -0.5 . These regions correspond to such initial conditions for which the electron and hole trajectories will only be slightly different, but this nearly periodic orbit will slowly drift in phase space[10, 20] [see also Fig. 4(b)]. This dynamics resembles the intermittent behavior in normal billiards[23] where this near-integrable motion usually evolves in the vicinity of tori or isolated periodic orbits. In the present case [Fig. 1(a)], however, it is a consequence of the retroreflection mechanism and is therefore a peculiarity of ABs. Nevertheless, owing to this drift either the electron or the hole trajectory will eventually reach the edge of the N-S interface and then by hitting the normal wall instead of the superconductor, escapes to the chaotic sea.

In what follows, we show how the properties of the classical phase space leave their fingerprints on the eigenstates of Andreev billiards. First, we briefly summarize the quantum treatment of the system. The spinor wavefunction $\psi(\mathbf{r}) = [u(\mathbf{r}), v(\mathbf{r})]^T$ (with $u(\mathbf{r})$ electron and $v(\mathbf{r})$ hole components) of the N-S hybrid systems satisfies the Bogoliubov-de Gennes equations $\hat{\mathcal{H}}\psi(\mathbf{r}) = \varepsilon\psi(\mathbf{r})$, where $\hat{\mathcal{H}} = \hat{\mathcal{H}}_0\sigma_z + \Delta(\mathbf{r})\sigma_x$, and $\hat{\mathcal{H}}_0 = -\hbar^2/2m\nabla^2 - \mu$ is the single-particle Hamiltonian with Dirichlet boundary conditions at the normal walls. Here μ is the chemical potential and σ_z, σ_x are Pauli matrices. We assume that the superconducting pair potential is $\Delta(\mathbf{r}) = \Delta_0$ constant inside the lead and zero in the N region[9]. The calculation of the wavefunction requires two steps: first we obtain the energy levels of the SA billiard using a quantum mechanically exact secular equation which can be derived invoking the scattering approach of Ref. [9]. The method also furnishes us with the wavefunction in the superconducting lead and at the N-S interface. Then the boundary integral method is employed to find the wavefunction in the normal dot[18]. We work in the regime $\delta_N \ll E_T \ll \Delta_0 \ll E_F$ [9] where δ_N is the mean level spacing of the isolated normal dot and E_T is the Thouless energy[27].

The classical-quantal correspondence of phase space structures and eigenstates of a given system can be studied with the help of the Wigner function[21]. In order to compare the Wigner function with the PS, we calculated the projection of the Wigner function[26] of both the electron and the hole components of the wavefunction onto the PS:

$$\mathcal{W}_P(y, p_y) = \frac{1}{2\pi\hbar} \int dY e^{-ip_y Y} \zeta^*(x, y - \frac{Y}{2}) \zeta(x, y + \frac{Y}{2}) \quad (1)$$

evaluated at the N-S interface (ie $x = 0$), ζ is either $u(\mathbf{r})$ or $v(\mathbf{r})$ and p_y is the parallel (to the interface) component of the momentum. The Wigner function is not positive definite and usually exhibits rapid oscillations

that can obscure the physical content. For this reason, like in Ref. [26], we smoothed the projection \mathcal{W}_P with a Gaussian, which was chosen narrower than the minimum uncertainty Gaussian. Note that \mathcal{W}_P is symmetric in p_y , since the system is time reversal invariant. This symmetry is absent in the Poincaré map, because incidental electrons (holes) are not taken into account.

In common with normal billiards, most of the eigenstates of the SA billiards can be classified as ‘chaotic’ or ‘regular’ [24, 25, 26]. The chaotic eigenstates can further be subdivided into two groups: i) ergodic-like, and ii) scarred states. Regarding the regular states, they either can be associated with the intermittent-like regions of the phase space or with quantized tori. We now consider each case.

For ergodic-like eigenstates (an example is shown in Fig. 2(a)) both the electron and the hole components

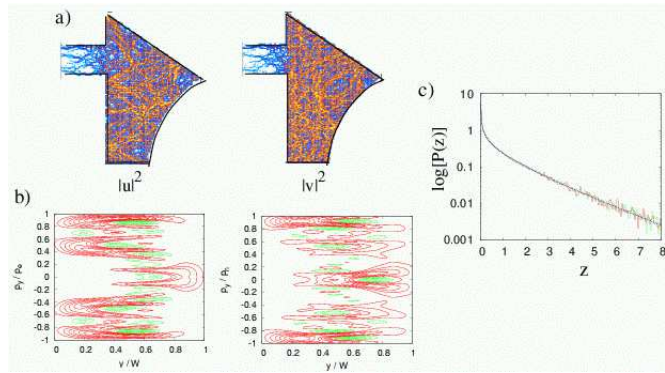


FIG. 2: (color online) The probability densities of the electron ($|u|^2$) and hole ($|v|^2$) components of a chaotic eigenstate ($\varepsilon/\Delta_0 = 0.060395$) of the SA billiard (a). The corresponding smoothed projections of the Wigner function onto the PS (b) in units of y/W and p_y/p_e , p_y/p_h for the electron and hole components respectively. Here $p_e = mv_e$ and $p_h(\varepsilon) = p_e(-\varepsilon)$. Eight equally spaced positive contours (red lines) and five negative contours (green lines) are plotted. The distribution of the scaled probabilities z_e (red line), z_h (green line) and the Porter-Thomas distribution (blue line) (c).

of the wavefunction seems to cover the normal dot in a roughly uniform way. Nevertheless, they display different interference pattern which translates also into the corresponding projections of the Wigner functions. Examining Fig. 1(a) and Fig. 2(b) one can see that \mathcal{W}_P has high amplitude in such regions, which corresponds to chaotic regions in the PS. This observation is reinforced by the good agreement between the probability distribution of the scaled local densities $z_e(\mathbf{r})$, $z_h(\mathbf{r})$ and the Porter-Thomas distribution $\mathcal{P}(z) = 1/\sqrt{2\pi}z \exp(-z/2)$ shown in Fig. 2(c). Here $z_e(\mathbf{r}) = (\mathcal{A}/\mathcal{N}_e)|u(\mathbf{r})|^2$, where $\mathcal{N}_e = \int |u(\mathbf{r})|^2 d^2\mathbf{r}$, and the integration is performed over the area \mathcal{A} of the normal dot (an analogous definition applies for the hole density $z_h(\mathbf{r})$). Both the electron and the hole components of chaotic eigenstates of ABs can thus be considered, similarly to the eigenstates of chaotic normal billiards[21, 22], as being a superposition of infi-

nite number of plane waves with fixed wave number, but with random directions and amplitudes.

The old wisdom of the quantum chaos: ‘the scars are scarce’ seems to hold also for ABs. Out of 99 eigenstates

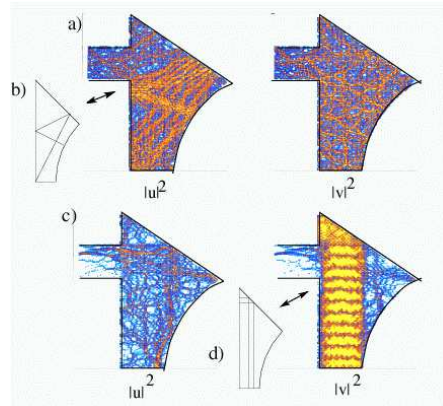


FIG. 3: (color online) The probability densities of the electron ($|u|^2$) and hole ($|v|^2$) components of a scarred eigenstate ($\varepsilon/\Delta_0 = 0.88323$) of the SA billiard (a) and the corresponding unstable periodic orbit (b). The probability densities of a decoupled state at $\varepsilon/\Delta_0 = 0.42901$ (c) and the marginally stable periodic orbit family over which the hole component shows enhancement (d).

of the system with geometrical parameters listed in the caption of Fig. 1(a), only 2 can be classified as scarred, one of them is shown in Fig. 3(a) along with the periodic orbit that scars the electron component (Fig. 3(b)). We call these states ‘genuine Andreev-scarred’ to distinguish them from the other type of states which are decoupled from the superconductor[13] and in certain cases also show enhancement over periodic orbits (see Figs. 3(c) and (d)). In the case of decoupled eigenstates the amplitude of the wavefunction at the N-S interface is small and the probability of finding the quasiparticle in either the electron or hole state inside the dot is enhanced. For the example shown in Fig. 3(d), integrating $|v(\mathbf{r})|^2$ over the area of the billiard one finds that this probability is 91% whereas only 7% for the electron component (and 2% corresponds to the probability of quasiparticles in the superconductor). In contrast, for the eigenstate shown in Fig. 3(a) the wavefunction has an apparently finite value at the N-S interface and the probabilities are 56% (electrons) and 31% (holes).

Regarding the regions of regular motion, we found that both the intermittent-like parts of the phase space and the regular islands can give rise to quantum eigenstates. The electron and the hole components of regular eigenstates display very similar interference patterns and the probabilities of the electron and hole state in the dot have close values. Furthermore, the localization of both the eigenfunction and the corresponding smoothed \mathcal{W}_P onto the underlying phase space structure can be observed. As for the islands of stability shown in Fig. 1(a), they enclose a very small area and thus for the numerically ac-

cessible wavelengths they are not resolved quantum mechanically. A much more amenable system for studying the correspondence between quantum eigenstates and a regular island can be obtained by attaching the superconducting lead at $h = 0$, since in this case the emerging regular island is larger [see Fig. 1(b)]. Our findings on the

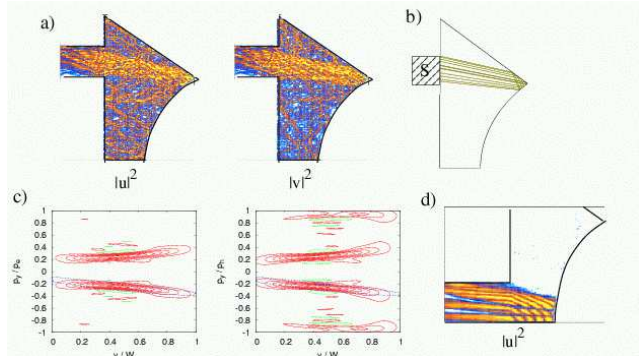


FIG. 4: (color online) The probability density of the electron ($|u|^2$) and hole ($|v|^2$) components of an intermittent eigenstate ($\varepsilon/\Delta_0 = 0.44652$) of the SA billiard (a). One of the slowly drifting electron-hole orbits during the intermittent-like motion (b) which form the regular strip around $v_y/v_e \approx -0.2$ in Fig. 1(a). The orbit comprises electron (red) and hole (green) trajectories. The smoothed projections \mathcal{W}_P for the electron and the hole components of the eigenstate (c). Eight equally spaced positive contours (red lines) and one negative contour (green line) are plotted. The blue curve marks the location of that region of the PS, in which the drifting electron-hole orbits, like that one in Fig. 4(b), stay longer than τ_H (see text). The electron component of a wavefunction localized onto a quantized torus when $h = 0$ (d). The hole component is almost identical and thus not shown here.

eigenfunction properties listed above are based on studying this case [see also Fig. 4(d)], which is, however, not treated here in more detail for the lack of space. Finally, we found that as expected, those intermittent-like regions support quantum eigenstates, which correspond to staying times longer than the Heisenberg time $\tau_H = 2\hbar/\delta_N$. An example is shown in Fig. 4(a), while Fig. 4(c) shows that the smoothed \mathcal{W}_P also has high amplitude in the corresponding region.

In summary, we investigated the quantal-classical correspondence in Andreev billiards with a chaotic normal dot. We showed that in contrast to the common belief, the interplay of critical points and non-exact velocity reversal can render the classical dynamics non-integrable even for zero magnetic field. It was also shown that the eigenstates of the system can be classified as chaotic or regular corresponding to different regions of phase space. This implies that while the retracing approximation has been proved to be useful in understanding the energy dependence of the density of states [13, 17], it may not be adequate when addressing the properties of individual eigenstates. Experimentally, the eigenstates of the Andreev billiards might be studied using scanning tunneling probe, and those which comprise quasiparticle density en-

hancement in certain part of the dot should be discernible from the ergodic ones.

We would like to thank C. W. J. Beenakker, P. G. Silvestrov and H. Schomerus for useful discussions. This work is supported by E. C. Contract No. MRTN-CT-2003-504574, EPSRC, the Hungarian-British TeT, and the Hungarian Science Foundation OTKA TO34832.

* Electronic address: kor@complex.elte.hu

- [1] E. J. Heller, Phys. Rev. Lett. **53**, 1515 (1984).
- [2] E. G. Vergini, J. Phys. A: Math. Gen. **37**, 6507 (2004); E. Bogomolny and C. Schmit, Phys. Rev. Lett. **92**, 244102 (2004).
- [3] J. P. Bird *et al.*, Phys. Rev. Lett. **82**, 4691 (1999); Y. Takagaki and K. H. Ploog, Phys. Rev. E **62**, 4804 (2000); R.G. Nazmitdinov *et al.*, Phys. Rev. B **66**, 085322 (2002); R. Crook *et al.*, Phys. Rev. Lett. **91**, 246803 (2003); B. Weingartner *et al.*, cond-mat/0504344; M. Hentschel and K. Richter, Phys. Rev. E **66**, 056207 (2002); S.-Y. Lee *et al.*, Phys. Rev. Lett. **93**, 164102 (2004).
- [4] A. P. S. de Moura *et al.*, Phys. Rev. Lett. **88**, 236804 (2002).
- [5] A. Bäcker *et al.*, Phys. Rev. E **66**, 016211 (2002).
- [6] Y.-H. Kim *et al.*, Phys. Rev. B **65**, 165317 (2002).
- [7] R. Akis *et al.*, Appl. Phys. Lett. **81**, 129 (2002); D. K. Ferry *et al.*, Phys. Rev. Lett. **93**, 026803 (2004).
- [8] I. Kosztin *et al.*, Phys. Rev. Lett. **75**, 1735 (1995).
- [9] C. W. J. Beenakker, Lect. Notes Phys. **667**, 131 (2005); cond-mat/0406018.
- [10] P. G. Silvestrov *et al.*, Phys. Rev. Lett. **90**, 116801 (2003).
- [11] M. C. Goorden *et al.*, Phys. Rev. B **68**, 220501(R) (2003).
- [12] Ph. Jacquod *et al.*, Phys. Rev. Lett. **90**, 207004 (2003).
- [13] F. Libisch *et al.*, cond-mat/0504098 (to be published in Phys. Rev. B).
- [14] N. G. Fytas *et al.*, cond-mat/0504322.
- [15] A. F. Andreev, Zh. Eksp. Theor. Fiz. **46**, 1823 (1964) [Sov. JETP. **19**, 1228 (1964)].
- [16] J. Wiersig, Phys. Rev. E **65**, 036221 (2002).
- [17] J. A. Melsen *et al.*, Europhys. Lett. **35** 7 (1996).
- [18] Details of the calculations will be given elsewhere.
- [19] A. Kormányos *et al.*, Phys. Rev. B **70**, 052512 (2004).
- [20] M. Stone, Phys. Rev. B **54**, 13222 (1996); A. V. Shytov *et al.*, Soviet Physics Uspekhi (Usp. Fiz. Nauk) **168** (2), 222 (1998) (cond-mat/9709329).
- [21] M. V. Berry, in *Les Houches Lecture Series, Session XXXVI*, North Holland, Amsterdam, 171-271 (1983).
- [22] H. Ishio *et al.*, Phys. Rev. E **64**, 056208 (2001); J. D. Urbina and K. Richter, J. Phys. A: Math. Gen. **36**, L495 (2003).
- [23] P. Dahlqvist, J. Phys. A: Math. Gen. **25**, 6265 (1992); S. D. Frisch and E. Doron, J. Phys. A: Math. Gen. **30**, 3613 (1997).
- [24] I. C. Percival, J. Phys. B: At. Mol. Phys. **6**, L229 (1973).
- [25] O. Bohigas *et al.*, Phys. Rep. **223** 43 (1993).
- [26] T. Prosen and M. Robnik, J. Phys. A: Math. Gen. **26**, 5365 (1993); G. Veble *et al.*, *ibid* **32**, 6423 (1999).
- [27] The value of ε/E_F is 0.0069 for Figs. 1(a,b). Throughout this paper the number of open channels in the lead is $k_F W/\pi = 25.51$ (k_F is the Fermi wavenumber), while

$\Delta_0/E_F = 0.015$ and $W = 0.21$, $R = 0.8$.